Electronic Supplementary Information (ESI)

Ethene Hydrogenation vs. Dimerization over a Faujasite-Supported $[Rh(C_2H_4)_2]$ Complex. A Computational Study of Mechanism

Agalya Govindasamy,[a] Velina K. Markova,[a] Alexander Genest,[a] Notker Rösch[a,b,]*

[a] Institute of High Performance Computing, Agency for Science, Technology and Research, 1 Fusionopolis Way, #16-16 Connexis, Singapore 138632, Singapore

[b] Department Chemie and Catalysis Research Center, Technische Universität München, 85747 Garching, Germany.

Content

Section S1 The location of the di-ethlylene Rh(I) complex in the faujasite framework..... S2

Section S2 Alternative pathways for the dimerization of ethene in the $[Rh(C_2H_4)_2]^+$ complex..... S5

Section S3 Free energy profiles of the alternative pathways for the hydrogenation of ethene over a di-ethene Rh(I) complex..... S7

Section S4 Total energies, relative energies and free energies of reactants, transition structures, and products..... S8

Section S5 Calculated structural parameters of reactants, transition states. and products... S9

Section S6. The 5T cluster model used for the partial normal mode analysis..... S24

Section S7 Cartesian coordinates of all intermediates and transition states S24

* Corresponding author. Email: roesch@mytum.de

Section S1 The location of the di-ethlylene Rh(I) complex in the faujasite framework

The faujasite (FAU) zeolite framework (Figure S1) is represented in this study as an ideal periodic model. To elucidate the impact of the dispersion interaction on the lattice parameters, we optimized the silicalite triclinic unit cell (Figure S2) at the PBE level, both without and with the D2 corrections, Table S1. With just the PBE functional, the lattice parameters are overestimated by 0.9% and the cell volume by 2.6%, compared to the corresponding experimental values.[1] At the PBE-D2 level, these key structure characteristics are overestimated by 0.6% and 1.9%, respectively. Obviously, the cell parameters from the PBE-D2 calculation agree better with the experimental values (Table S1). The DFT-D2 strategy has been shown to yield accurate adsorption energies in systems with notable van der Waals interactions.[2-4] All calculations of this study were carried out at the PBE-D2 level.

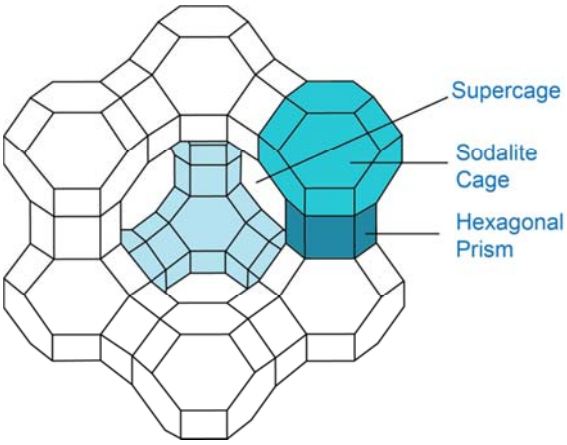

Figure S1. Sketch of the faujasite framework.

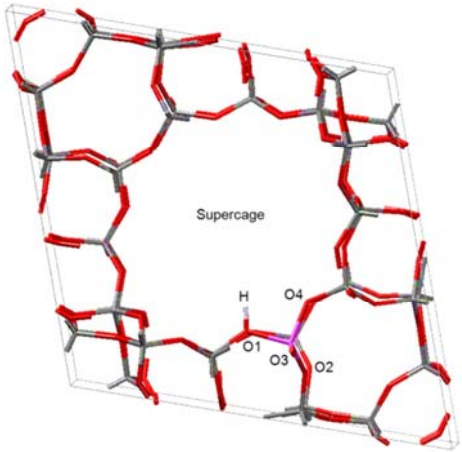

Figure S2. Structure of the triclinic unit cell of the faujasite model with 48T atoms, employed for the periodic DFT calculations.

One of the T atoms in the primitive cell model of the silicalite was substituted by an Al atom representing the framework ratio of the Si/Al = 47 (exp. ratio Si/Al = 30). The resulting net negative charge of the lattice was compensated by a proton. The charge-neutralizing proton can bind to any one of the four distinct oxygen centers present in the FAU. We calculated the relative stability of the proton sites as O3–H $\simeq$ O1–H > O2–H > O4–H. The relative energy difference of O1–H, O2–H and O4–H with respect to the most stable O3–H moiety are 0.6 kJ mol^{-1}, 6.3 kJ mol^{-1}, and 8.7 kJ mol^{-1}, respectively. The introduction of such a *Brønsted* acid site is known to enlarge the unit cell volume by 13 Å^3 (~0.35%), reflecting the difference in volume of the SiO_4 and $AlO_3(OH)$ T sites.[5] The re-optimized cell parameters of the Al-substituted FAU model was calculated to be enlarged by 18 Å^3 (~0.5%), compared to the silicalite model, Table S1.

Table S1. Lattice parameters[a] of the triclinic unit cell of the silicalite model, calculated with various computational approaches. Data for HY from experiment shown for comparison.

Zeolite	Functionals	*a*	*b*	*c*	*V*
Silicalite	PW91	1736	1736	1736	3.700
	PBE	1737	1737	1737	3.703
	PBE-D2	1732	1732	1732	3.675
	Exp.[b]	1722	1722	1722	3.607
HY[c]	PBE-D2	1733	1734	1737	3.693

[a] Lengths of unit cell vectors *a*, *b*, *c* (pm) and volume *V* (nm^3) of the unit cell. [b] Ref.1.
[c] Lattice parameters of HY for systems where the proton is attached to the O1 oxygen site.

We explored the stability of several adsorption complexes of $[Rh(C_2H_4)_2]^+$ where the zeolite lattice formally acts as bidentate ligand. To this end, we selected two sets of bidentate binding sites of the zeolite framework. In the first set (O1O2, O2O4, and O1O4), the two oxygen centers of the bidentate site are directly bonded to the Al T-site, Figure S3. Adsorption of the Rh complex on sites involving O3 ultimately lead to a structure where the Rh complex adsorbs on the O1O4 site, likely due to a steric repulsion from the zeolite wall. Site O1O4 is located at the 12-MR window of the supercage, whereas the sites O1O2 and O2O4 are situated at a four-member ring (4-MR) of D6R and a six-member ring (6-MR) of SOD, respectively, Figure S1. In the second set, one oxygen center binds directly to the Al T-site, as in the first set. The other oxygen center is remote to the Al site, binding to a Si atom

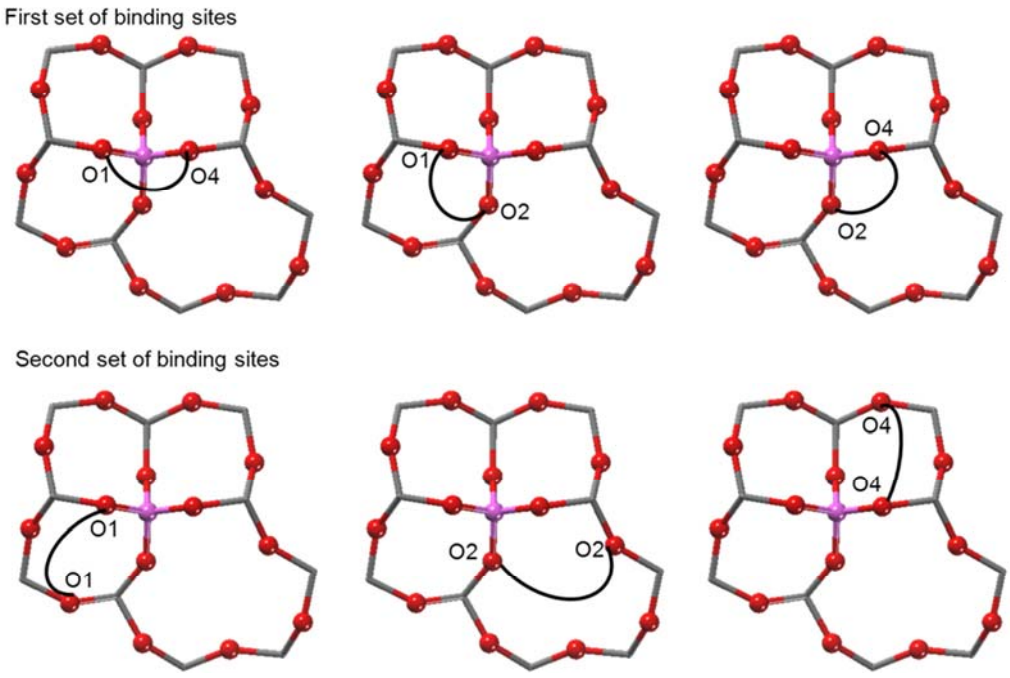

Figure S3. Bidentate binding sites in faujasite considered for the adsorption of $[Rh(C_2H_4)_2]^+$.

Table S2. Calculated reaction free energies G_r[a] (in kJ mol^{-1}; at 303 K and 1 atm) of $[Rh(C_2H_4)_2(acac)]$ with the acidic proton of faujasite leaving $[Rh(C_2H_4)_2]^+$ anchored at designated oxygen sites, and optimized Rh−O_z bond distances (pm).

Binding site[b]	G_r	Rh–O
O1O2	-37.25	223, 229
O1O4	-61.40	218, 225
O2O4	-47.42	223, 223
O1O1	-42.38	222, 233
O4O4[c]	-14.45	230, 256

[a] $G_r = G([Rh(C_2H_4)_2]/HY) + G(Hacac) - G(HY) - G([Rh(C_2H_4)_2(acac)])$; see Eq. (1) of the main text. [b] Bidentate binding sites of the fragment $Rh(C_2H_4)_2$ complex in faujasite. A Rh complex initially located at site O2O2 moves to site O2O4 during optimization. [c] A Rh complex initially located at site O4O4 leads to monodentate adsorption at a single O4 site.

immediately adjacent to the Al center. We explored the binding sites O1O1, O2O2, and O4O4; see Figure S3. Site O1O1 is part of the 4-MR of D6R, while the sites O2O2 and O4O4 are part of the 6-MR and the 4-MR of the SOD cage, respectively (Figure S1).

The reaction energies calculated according to Eq. (1) of the main text (Table S2) reveal that the cationic species $[Rh(C_2H_4)_2]^+$ prefers to bind with G_r = -61.4 kJ mol^{-1} at site O1O4, i.e., on the 12-MR window of the supercage. The reaction energies (in absolute terms) for the adsorption of $[Rh(C_2H_4)_2]^+$ at the other sites decrease in the order O1O4 > O2O4 > O1O1 > O1O2 > O4O4. The second-most stable complex, at site O2O4, lies about 14 kJ mol^{-1} higher in energy. Adsorption site O1O1 has a similar stability (weaker by 5 kJ/mol), but one of the Rh-O distance is longer and reaches 233 pm, Table S2. In the two most stable adsorption complexes, the fragment $[Rh(C_2H_4)_2]^+$ binds to the framework in an asymmetric fashion, with the two Rh–O distances differing by ~6 pm, Table S2. In the two remaining cases, the adsorbed fragment altered its location during optimization, namely from O2O2 to O2O4 and from O4O4 to a monodentate structure at the O4 site near Al (G_r = -14.5 kJ mol^{-1}, Rh–O4= 230, 256 pm).

1 C. Baerlocher, L. B. McCusker and D. H. Olson, Atlas of zeolite framework types, Elsevier **2007**; http://www.iza-structure.org/databases;

2 C. M. Nguyen, M. F. Reyniers and G. B. Marin, *Phys. Chem. Chem. Phys.* **2010**, 12, 9481-9493.

3 J. Van der Mynsbrugge, K. Hemelsoet, M. Vandichel, M. Waroquier and V. Van Speybroeck, *J. Phys. Chem. C* **2012**, 116, 5499-5508.

4 C.-c. Chiu, G. N. Vayssilov, A. Genest, A. Borgna and N. Rösch, *J. Comput. Chem.* **2014**, 35, 809-819.

5 A. P. Ugliengo, B. Civalleri, C. M. Zicovich-Wilson , R. Dovesi, *Chem. Phys. Lett.* **2000**, *318*, 247-255.

Section S2 Alternative pathways for the dimerization of ethene in the $[Rh(C_2H_4)_2]^+$ complex

The dimerization of ethene on the supported $[Rh(C_2H_4)_2]^+$ complex was studied also in the absence of hydrogen. Figure S4 shows the energy profiles of these two alternative pathways. The oxidative C-C coupling of the two π-bonded ethene ligands in the initial complex, **1→15**, is characterized by the highest activation energy of all dimerization pathways studied – 150 kJ mol^{-1} (Figure S4). Moreover, this process is highly endergonic. The other two dimerization pathways without any adsorbed hydrogen, **1-20** and **1-25**, start from the hydride-vinyl complex $[Rh(C_2H_4)(H)(C_2H_3)]^+$ **16**, which is obtained via H abstraction by Rh from one ethene ligand (**1→16**). The subsequent steps **16→17** and **16→21** exhibit low barriers of 7 kJ mol^{-1} and 10 kJ mol^{-1}, respectively. Reaction **16→17** is an H addition to the other ethene ligand forming the ethyl-vinyl complex **17**. The transferred H atom of **17** undergoes an agostic interaction with the Rh center, Rh-H1 = 169 pm (Table S4).

A slightly exergonic rotation of the ethene ligand in **16** leads to complex **21**. The metal center of **22** is very low coordinated and the adsorption **22→23** of an ethene molecule precedes the formation of butene; the reaction free energy of this attachment is -34 kJ mol^{-1}. Subsequently, H adds to the butylene species, ΔG_r = -95 kJ mol^{-1}. In this step, **23→24**, a barrier of 42 kJ mol^{-1} has to be overcome, Figure S4. One more ethene unit has to be attached, **24→25**, with ΔG_r = 8 kJ mol^{-1}, followed by the elimination **25→1** of the product, which is exergonic by 9 kJ mol^{-1}. Ultimately, the initial Rh complex **1** is reconstituted.

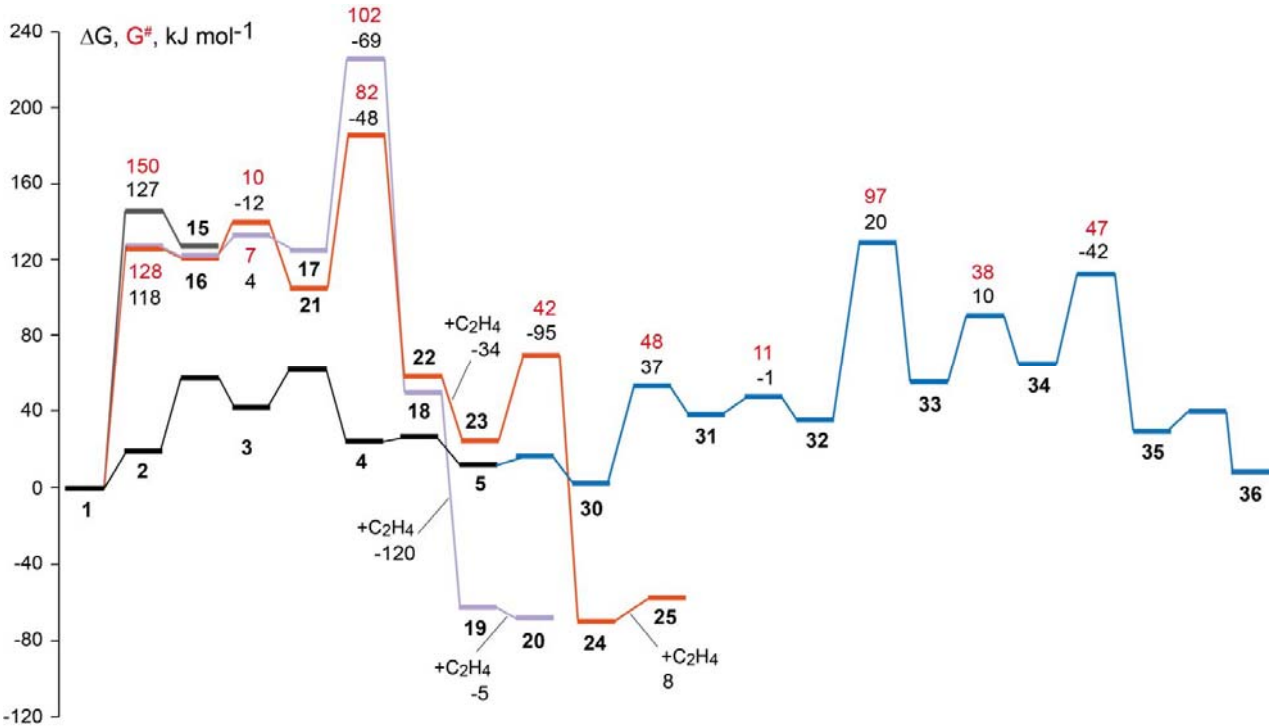

Figure S4. Free energy profile of alternative pathways to ethene dimerization in the supported complex $[Rh(C_2H_4)_2]^+$ *in the absence* of hydrogen; see (Figure 3. Pathways **1-15**, **1-16-17-20** and **1-16-21-25** shown in grey, purple and light red, respectively. The main dimerization pathway (blue) is presented for comparison; see Figure 5.

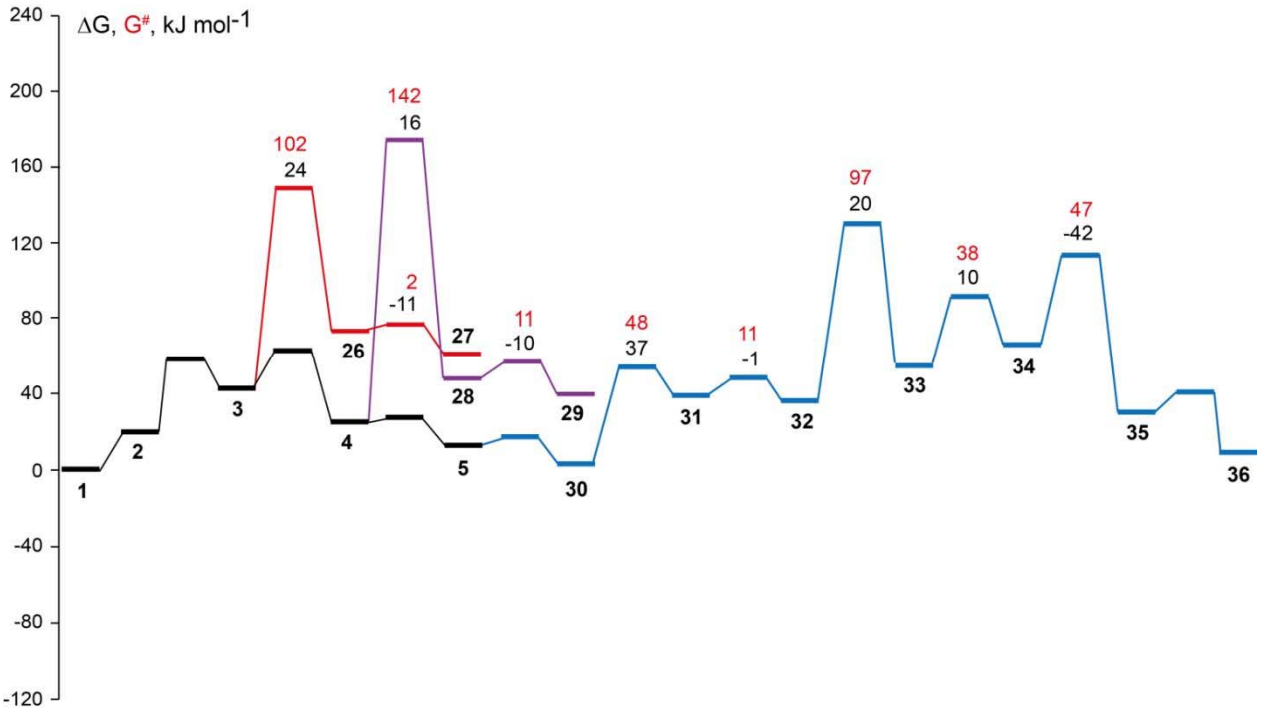

Figure S5. Free energy profile of alternative ethene dimerization in the supported complex $[Rh(C_2H_4)_2(H_2)]^+$ *in the presence of hydrogen* – pathways **1-3-26-27** (red) and **1-4-28-29** (purple). The main dimerization pathway (blue) is presented for comparison; see Figure 5.

Section S3 Free energy profiles of the alternative pathways for the hydrogenation of ethene over a di-ethene Rh(I) complex

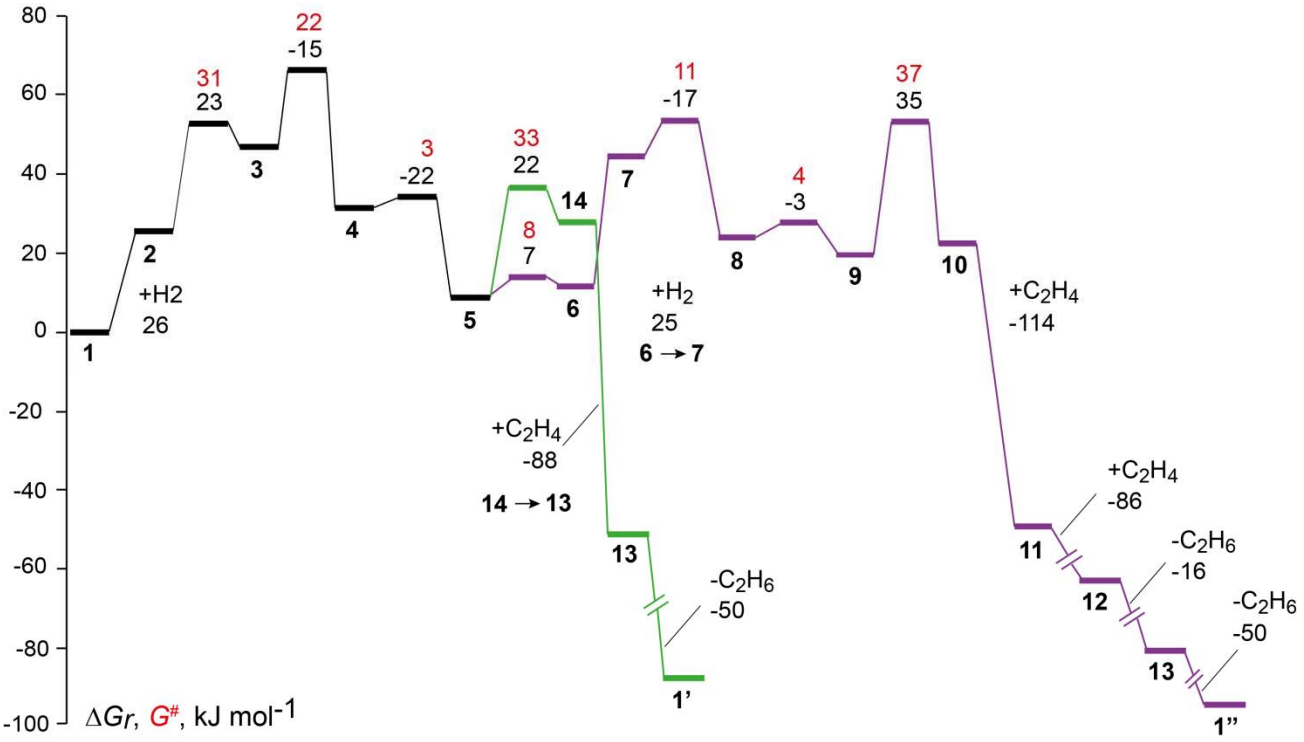

Figure S6. Free energy profiles of alternative pathways to the hydrogenation of ethene over the faujasite-supported complex $[Rh(C_2H_4)_2]^+$, via monoethyl (**5-14-13**, green) or the diethyl moiety **6** (**5-6-13**, purple). Same lay-out as Figure 5 of the main text.

Section S4 Total energies, relative energies and free energies of reactants, transition structures, and products

Table S3. Total energies (eV) of the reactants, transition states and products, ΔE and ΔG values are relative reaction values in kJ mol^{-1} with respect to Complex **1** and appropriate numbers of hydrogen, ethene or ethane moieties.

Complex	Total Energy	ΔE	ΔG	Complex	Total Energy	ΔE	ΔG
H_2	-6.759			**24**	-1253.536	-137.1	-71.3[g]
C_2H_4	-31.998			**25**	-1285.865	-169.1	-63.0[h]
C_2H_6	-40.554			TS **1-16**	-1218.632	143.2	128.2[f]
C_4H_8	-65.325			**16**	-1218.724	134.4	117.7[f]
1	-1220.117	0.0	0.0	**TS 16-17**	-1218.601	146.2	124.3[f]
2	-1226.976	-9.7	26.5[a]	**17**	-1218.673	139.3	121.6[f]
TS **2-3**	-1226.765	10.7	57.8[a]	TS **17-18**	-1217.601	242.7	224.0[f]
3	-1226.836	3.8	49.5[a]	**18**	-1219.571	52.6	52.8[f]
TS **3-4**	-1226.641	22.6	71.1[a]	**19**	-1253.427	-126.6	-66.8[g]
4	-1227.042	-16.1	34.3[a]	**20**	-1286.207	-202.1	-71.5[h]
TS **4-5**	-1227.014	-13.4	36.9[a]	TS **3-26**	-1225.810	102.9	151.2[a]
5	-1227.265	-37.6	11.8[a]	**26**	-1226.635	23.2	73.6[a]
TS **5-6**	-1227.161	-27.5	19.6 [a]	TS **26-27**	-1226.634	23.3	76.0[a]
6	-1227.182	-29.5	18.6 [a]	**27**	-1226.826	4.8	62.9[a]
7	-1234.034	-38.5	43.4[b]	TS **4-28**	-1225.569	126.1	176.5[a]
TS **7-8**	-1234.012	-36.4	53.9[b]	**28**	-1226.945	-6.7	50.4[a]
8	-1234.430	-76.7	26.3[b]	TS **28-29**	-1226.786	8.6	61.2[a]
TS **8-9**	-1234.342	-68.2	30.6[b]	TS **5-30**	-1227.252	-36.4	14.4[a]
9	-1234.546	-87.9	22.8[b]	**30**	-1227.407	-51.2	0.2[a]
TS **9-10**	-1234.163	-51.0	60.0[b]	TS**30-29**	-1225.897	94.4	147.8[a]
10	-1234.192	-53.8	57.3[b]	**29**	-1227.085	-20.2	40.8[a]
11	-1268.023	-230.6	-57.1[c]	TS **30-31**	-1226.863	1.2	47.9[a]
12	-1301.865	-408.6	-142.6[d]	**31**	-1226.993	-11.3	37.3[a]
13	-1260.996	-378.2	-159.0[e]	TS **31-32**	-1226.890	-1.4	48.7[a]
TS **5-14**	-1226.978	-9.9	45.0[a]	**32**	-1227.007	-12.7	36.6[a]
14	-1227.171	-28.5	33.4[a]	TS **32-33**	-1226.077	77.0	133.3[a]
TS **1-15**	-1218.512	154.8	150.1[f]	**33**	-1226.876	0.0	56.2[a]
15	-1218.731	133.7	126.8[f]	TS **33-34**	-1226.480	38.2	94.0[a]
TS **1-16**	-1218.632	143.2	128.2[f]	**34**	-1226.813	6.1	66.2[a]
16	-1218.724	134.4	117.7[f]	TS **34-35**	-1226.258	59.6	113.5[a]
TS **16-21**	-1218.631	143.4	127.3[f]	**35**	-1227.146	-26.1	24.5[a]
21	-1218.852	122.0	105.7[f]	TS **35-36**	-1227.059	-17.7	31.8[a]
TS **21-22**	-1217.996	204.7	187.5[f]	**36**	-1227.379	-48.6	-1.5[a]
22	-1219.421	67.1	57.6[f]	**37**	-1260.506	-157.5	-46.2[i]
23	-1252.471	-34.4	23.3[g]	**38**	-1293.203	-224.9	-67.4[j]
TS **23-24**	-1251.944	16.5	65.7[g]	**39**	-1286.354	-216.2	-95.8[k]

The references for calculating ΔE and the corresponding ΔG values, when forming intermediates and transition states, are as follows:

[a] Complex **1** + H_2 [b] Complex **1** + $2H_2$ [c] Complex **1** + $2H_2$ + C_2H_4

[d] Complex **1** + $2H_2$ + $2C_2H_4$ [e] Complex **1** + $2H_2$ + $2C_2H_4$ – C_2H_6 [f] Complex **1**

[g] Complex **1** + C_2H_4 [h] Complex **1** + $2C_2H_4$ [i] Complex **1** + H_2 + C_2H_4

[j] Complex **1** + H_2 + $2C_2H_4$ [k] Complex **1** + $2C_2H_4$

Section S5 Calculated structural parameters of reactants, transition states. and products

Table S4. Structures and key geometric characteristics of reactants, transition states, and products. Distances in pm, angles in degree.

1	Rh-C1/C2	211/211	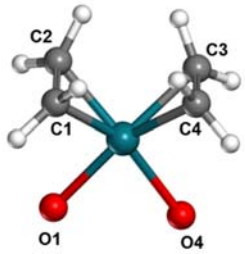
	Rh-C3/C4	211/211	
	Rh-O1/O4	218/225	
	C1-C2	141	
	C3-C4	141	
	C2-C3	289	
	Avg. O4-Rh-C1/C2	158	
	Avg. O1-Rh-C3/C4	159	
2	Rh-H1/H2	337/269	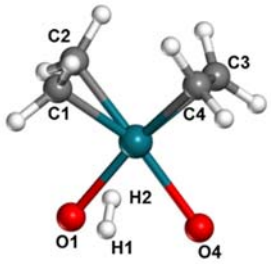
	Rh-C1/C2	211/211	
	Rh-C3/C4	211/211	
	Rh-O1/O4	219/223	
	C1-C2	141	
	C3-C4	141	
	H1-H2	76	
	Rh-H2-H1	151	
	Avg. O4-Rh-C1/C2	158	
	Avg. O1-Rh-C3/C4	159	
2-3	Rh-H1/H2	217/200	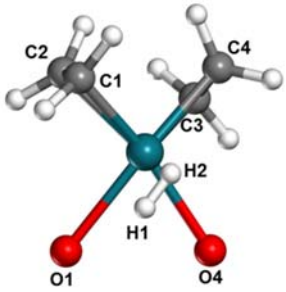
	Rh-C1/C2	212/212	
	Rh-C3/C4	210/210	
	Rh-O1/O4	234/224	
	C1-C2	141	
	C3-C4	143	
	H1-H2	78	
	Rh-H2-H1	92	
	Avg. O4-Rh-C1/C2	158	
	Avg. O1-Rh-C3/C4	145	
3	Rh-H1/H2	185/180	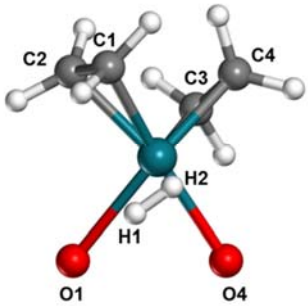
	Rh-C1/C2	214/211	
	Rh-C3/C4	211/215	
	Rh-O1/O4	240/225	
	C1-C2	141	
	C3-C4	142	
	C2-C3	299	
	H1-H2	83	
	Rh-H2-H1	80	
	H2-Rh-H1	26	
	Avg. O4-Rh-C1/C2	160	
	Avg. O1-Rh-C3/C4	108	

For TS **2**–**3**, only an approximate structure is available because the refinement by the dimer method failed.

3-4	Rh-H1/H2	169/165	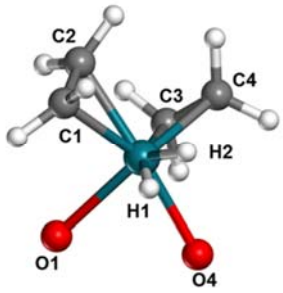
	Rh-C1/C2	215/215	
	Rh-C3/C4	220/219	
	Rh-O1/O4	238/219	
	C1-C2	140	
	C3-C4	141	
	H1-H2	99	
	H2-Rh-H1	34°	
	Avg. O4-Rh-C1/C2	158°	
	Avg. O1-Rh-C3/C4	106°	
4	Rh-H1/H2	158/154	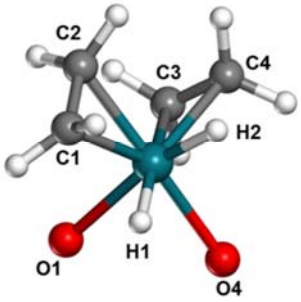
	Rh-C1/C2	214/212	
	Rh-C3/C4	231/230	
	Rh-O1/O4	232/221	
	C1-C2	141	
	C3-C4	137	
	C1-H1	201	
	C4-H2	240	
	H1-H2	203	
	H2-Rh-H1	81°	
	Avg. O4-Rh-C1/C2	159°	
	Avg. O1-Rh-C3/C4	97°	
4-5	Rh-H1/H2	161/154	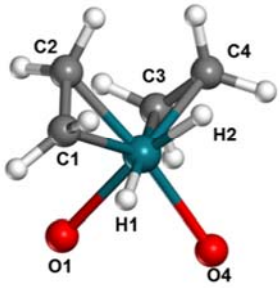
	Rh-C1/C2	215/208	
	Rh-C3/C4	226/226	
	Rh-O1/O4	231/226	
	C1-C2	144	
	C3-C4	138	
	C1-H1	167	
	H1-H2	208	
5	Rh-H1/H2	189/154	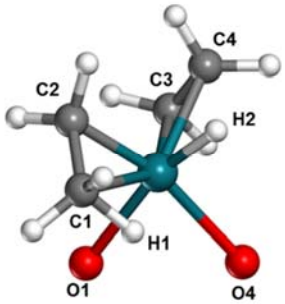
	Rh-C1/C2	234/203	
	Rh-C3/C4	213/215	
	Rh-O1/O4	228/235	
	C1-C2	150	
	C3-C4	141	
	C1-H1	118	
	C4-H2	206	
	C2-C3	309	
	C2-C4	334	
	C2-Rh-C3/C4	95°/107°	
5-6	Rh-H1/H2	199/160	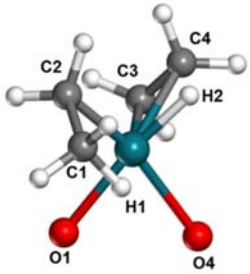
	Rh-C1/C2	241/202	
	Rh-C3/C4	207/216	
	Rh-O1/O4	221/236	
	C1-C2	151	
	C3-C4	144	
	C1-H1	116	
	C4-H2	148	

6	Rh-H1/H2	205/167	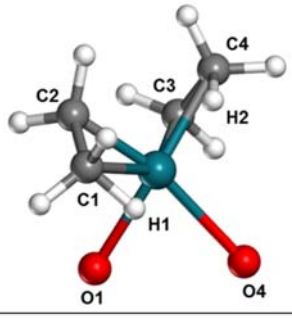
	Rh-C1/C2	245/202	
	Rh-C3/C4	205/219	
	Rh-O1/O4	218/237	
	C1-C2	151	
	C3-C4	146	
	C1-H1	115	
	C4-H2	130	
7	Rh-H1/H2	208/167	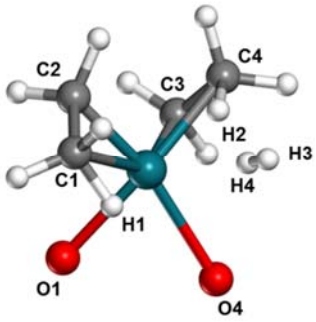
	Rh-H3/H4	382/309	
	Rh-C1/C2	247/202	
	Rh-C3/C4	205/219	
	Rh-O1/O4	218/238	
	C1-C2	151	
	C3-C4	146	
	C1-H1	115	
	C4-H2	129	
	H3-H4	75	
	Rh-H4-H3	164	
7-8	Rh-H1/H2	239/168	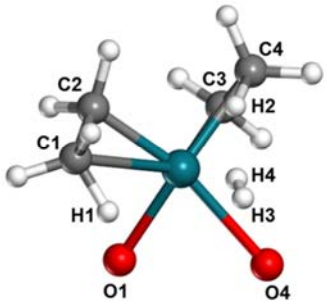
	Rh-H3/H4	342/274	
	Rh-C1/C2	265/202	
	Rh-C3/C4	203/219	
	Rh-O1/O4	216/238	
	C1-C2	152	
	C3-C4	147	
	C1-H1	112	
	C4-H2	128	
	H3-H4	76	
	Rh-H4-H3	155	
8	Rh-H1/H2	320/168	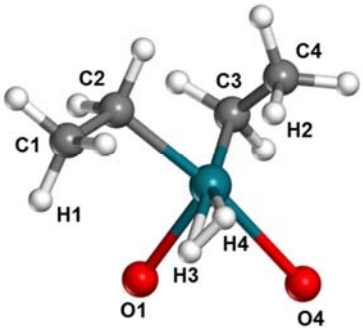
	Rh-H3/H4	184/179	
	Rh-C1/C2	302/207	
	Rh-C3/C4	207/222	
	Rh-O1/O4	220/240	
	C1-C2	152	
	C3-C4	146	
	C1-H1	110	
	C4-H2	130	
	C2-H3	277	
	C3-H4	377	
	H3-H4	83	
	Rh-H4-H3	80	
	H4-Rh-H3	26	

8-9	Rh-H1/H2	301/319	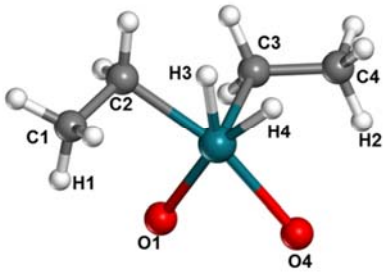
	Rh-H3/H4	155/156	
	Rh-C1/C2	294/213	
	Rh-C3/C4	206/299	
	Rh-O1/O4	227/224	
	C1-C2	152	
	C3-C4	151	
	C2-H3	161	
	C3-H4	256	
	H3-H4	132	
	H4-Rh-H3	50	
9	Rh-H1/H2	302/318	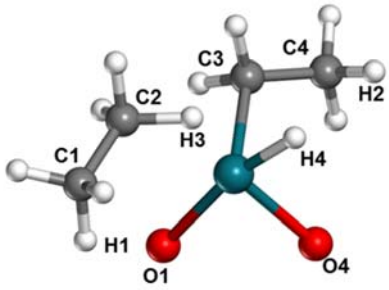
	Rh-H3/H4	169/154	
	Rh-C1/C2	314/234	
	Rh-C3/C4	205/300	
	Rh-O1/O4	233/213	
	C1-C2	152	
	C3-C4	151	
	C2-H3	120	
	C3-H4	249	
9-10	Rh-H3/H4	172/157	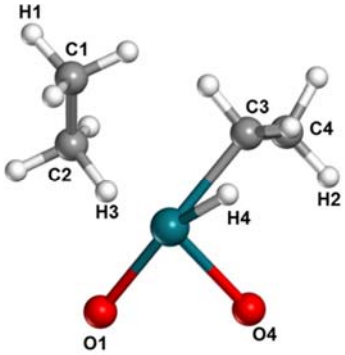
	Rh-C1/C2	353/236	
	Rh-C3/C4	217/292	
	Rh-O1/O4	219/216	
	C1-C2	153	
	C3-C4	152	
	C2-H3	119	
	C3-H4	144	
10	Rh-H3/H4	173/165	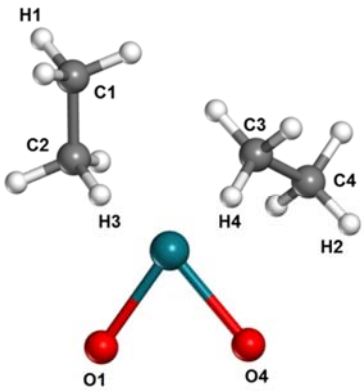
	Rh-C1/C2	352/235	
	Rh-C3/C4	227/298	
	Rh-O1/O4	215/216	
	C1-C2	153	
	C3-C4	153	
	C2-H3	119	
	C3-H4	126	
11	Rh-H1	169	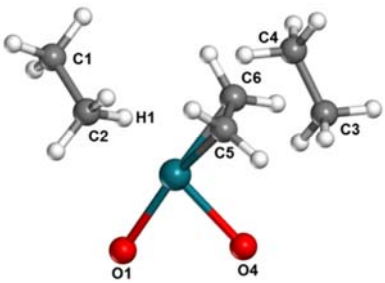
	Rh-C1/C2	366/239	
	Rh-C5/C6	210/210	
	Rh-O1/O4	216/218	
	C1-C2	154	
	C3-C4	153	
	C5-C6	141	
	C2-H1	119	

12	Rh-C5/C6	211/211	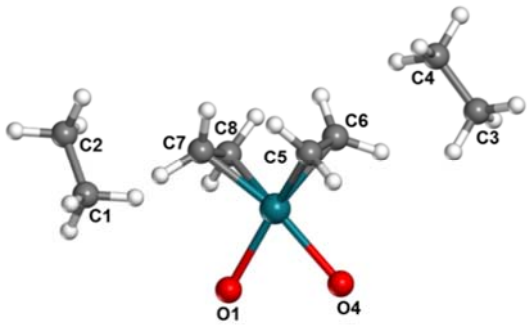
	Rh-C7/C8	211/211	
	Rh-O1/O4	218/225	
	C1-C2	153	
	C3-C4	153	
	C5-C6	141	
	C7-C8	141	
13	Rh-C5/C6	211/211	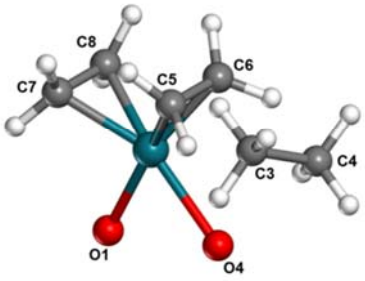
	Rh-C7/C8	211/211	
	Rh-C3/C4	354/432	
	Rh-O1/O4	218/226	
	C5-C6	141	
	C7-C8	141	
	C3-C4	153	
5-14	Rh-H1/H2	354/153	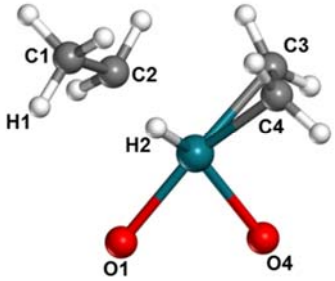
	Rh-C1/C2	331/215	
	Rh-C3/C4	211/212	
	Rh-O1/O4	218/225	
	C1-C2	154	
	C3-C4	141	
	C1-H1	110	
	C2-H2	161	
14	Rh-H1/H2	388/170	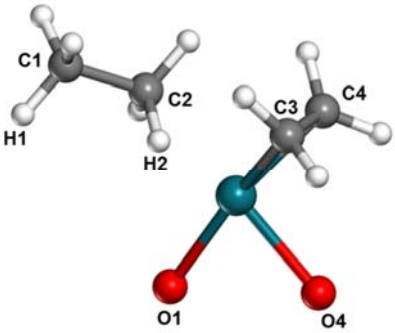
	Rh-C1/C2	365/238	
	Rh-C3/C4	210/210	
	Rh-O1/O4	218/217	
	C1-C2	154	
	C3-C4	142	
	C1-H1	110	
	C2-H2	120	
1-15	Rh-C1/C2	201/235	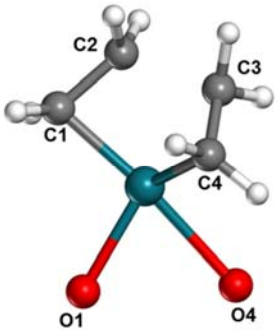
	Rh-C3/C4	223/202	
	Rh-O1/O4	213/239	
	C1-C2	147	
	C3-C4	147	
	C2-C3	189	

15	Rh-H1/H2	338/191	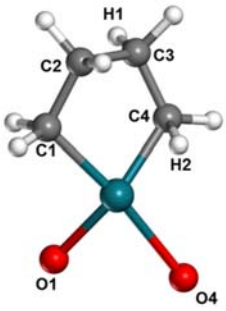
	Rh-C1/C2	206/294	
	Rh-C3/C4	293/191	
	Rh-O1/O4	207/235	
	C1-C2	153	
	C3-C4	150	
	C2-C3	153	
	C4-H2	122	
1-16	Rh-C1/C2	214/211	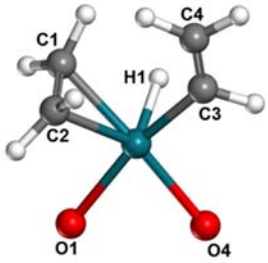
	Rh-C3/C4	200/305	
	Rh-O1/O4	226/223	
	C1-C2	141	
	C3-C4	134	
	C2-C3	295	
	C3-H1	194	
	Rh-H1	153	
	H1-Rh-C3	65	
	C2-C1-Rh-C3	89	
16	Rh-C1/C2	216/213	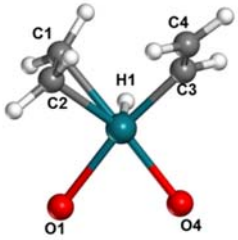
	Rh-C3/C4	199/291	
	Rh-O1/O4	229/218	
	C1-C2	140	
	C3-C4	134	
	C2-C3	289	
	C3-H1	236	
	Rh-H1	152	
	H1-Rh-C3	83	
	C2-C1-Rh-C3	-88	
16-17	Rh-H1	156	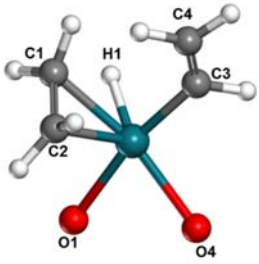
	Rh-C1/C2	214/207	
	Rh-C3/C4	198/303	
	Rh-O1/O4	232/219	
	C1-C2	143	
	C3-C4	134	
	C2-C3	301	
	C1-H1	163	
17	Rh-H1	168	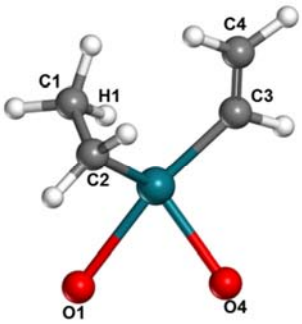
	Rh-C1/C2	220/203	
	Rh-C3/C4	198/302	
	Rh-O1/O4	231/214	
	C1-C2	147	
	C3-C4	134	
	C2-C3	298	
	C1-H1	127	

17-18	Rh-H1	169	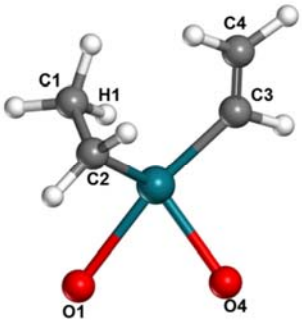
	Rh-C1/C2	219/217	
	Rh-C3/C4	207/289	
	Rh-O1/O4	216/220	
	C1-C2	150	
	C3-C4	136	
	C2-C3	181	
	C1-C2-C3-C4	50	
	C1-H1	125	
18	Rh-H1	172	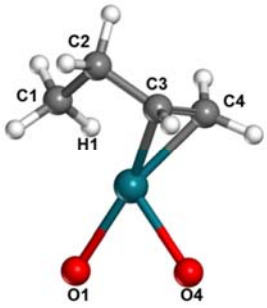
	Rh-C1/C2	228/274	
	Rh-C3/C4	209/210	
	Rh-O1/O4	217/215	
	C1-C2	155	
	C3-C4	142	
	C2-C3	152	
	C1-C2-C3-C4	65	
	C1-H1	121	
19	Rh-H1	319	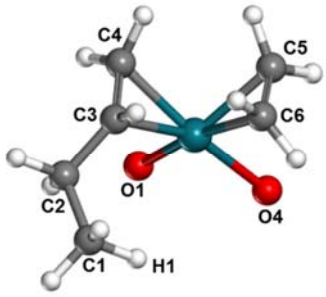
	Rh-C1/C2	361/299	
	Rh-C3/C4	213/210	
	Rh-C5/C6	209/211	
	Rh-O1/O4	228/222	
	C1-C2	153	
	C3-C4	141	
	C2-C3	151	
	C5-C6	142	
	C1-C2-C3-C4	160	
	C1-H1	110	
20	Rh-C1/C2	413/324	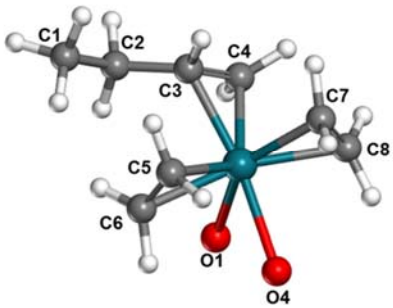
	Rh-C3/C4	219/212	
	Rh-C5/C6	224/226	
	Rh-C7-C8	212/216	
	Rh-O1/O4	246/227	
	C1-C2	153	
	C3-C4	141	
	C2-C3	151	
	C5-C6	139	
	C7-C8	142	
	C1-C2-C3-C4	180	

16-21	Rh-C1/C2	213/215	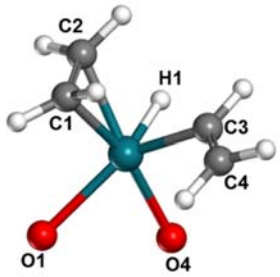
	Rh-C3/C4	199/288	
	Rh-O1/O4	232/217	
	C1-C2	140	
	C3-C4	133	
	C2-C3	294	
	C3-H1	222	
	Rh-H1	152	
	H1-Rh-C3	78	
	C1-C2-Rh-C3	-86	
21	Rh-C1/C2	212/214	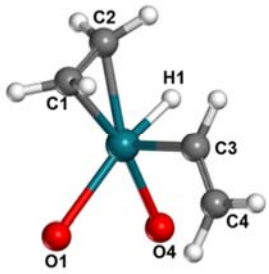
	Rh-C3/C4	197/289	
	Rh-O1/O4	231/217	
	C1-C2	141	
	C3-C4	133	
	C2-C3	294	
	C3-H1	237	
	Rh-H1	154	
	C1-C2-Rh-C3	-92	
	H1-Rh-C3	84	
21-22	Rh-C1/C2	202/230	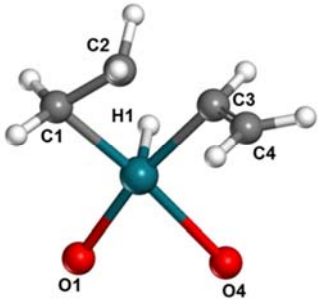
	Rh-C3/C4	210/302	
	Rh-O1/O4	214/242	
	C1-C2	147	
	C3-C4	135	
	C2-C3	181	
	C3-H1	253	
	Rh-H1	152	
	C1-C2-Rh-C3	178	
22	Rh-H1/H2	152/264	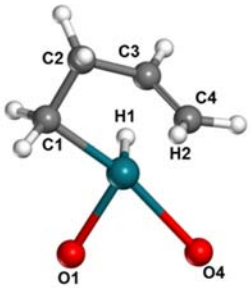
	Rh-C1/C2	206//277	
	Rh-C3/C4	217/213	
	Rh-O1/O4	217/243	
	C1-C2	152	
	C3-C4	140	
	C2-C3	159	
	C3-H1	234	
	C1-C2-C3-C4	-80	
23	Rh-C1/C2	210/277	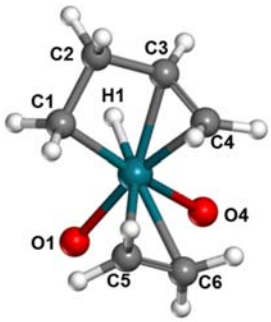
	Rh-C3/C4	216/213	
	Rh-C5/C6	233/233	
	Rh-O1/O4	221/245	
	C1-C2	153	
	C3-C4	141	
	C2-C3	152	
	C5-C6	137	
	C1-H1	240	
	Rh-H1	158	
	C1-C2-C3-C4	-64	

23-24	Rh-C1/C2	222/280	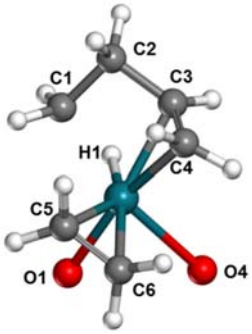
	Rh-C3/C4	216/215	
	Rh-C5/C6	219/222	
	Rh-O1/O4	219/253	
	C1-C2	153	
	C3-C4	140	
	C2-C3	152	
	C5-C6	140	
	C1-H1	162	
	Rh-H1	161	
	C1-C2-C3-C4	-89	
24	Rh-C1/C2	355/319	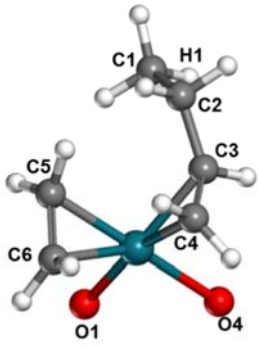
	Rh-C3/C4	214/211	
	Rh-C5/C6	211/209	
	Rh-O1/O4	219/228	
	C1-C2	153	
	C3-C4	141	
	C2-C3	150	
	C5-C6	141	
	C1-H1	110	
	Rh-H1	378	
	C1-C2-C3-C4	-140	
25	Rh-C1/C2	369/323	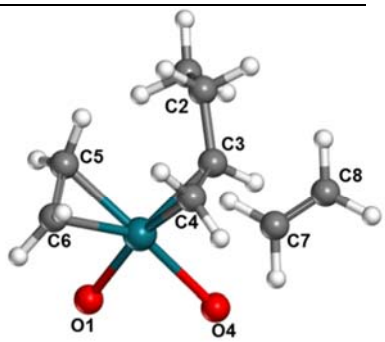
	Rh-C3/C4	215/210	
	Rh-C5/C6	211/210	
	Rh-C7/C8	384/462	
	Rh-O1/O4	219/227	
	C1-C2	153	
	C3-C4	141	
	C2-C3	150	
	C5-C6	141	
	C7-C8	133	
	C1-C2-C3-C4	-145	
3-26	Rh-H1/H2	172/167	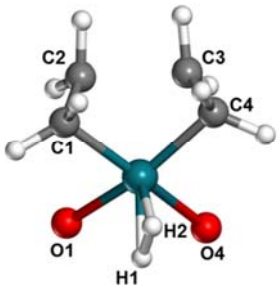
	Rh-C1/C2	204/227	
	Rh-C3/C4	225/205	
	Rh-O1/O4	231/243	
	C1-C2	146	
	C3-C4	146	
	C2-C3	206	
	H1-H2	90	
	Rh-H2-H1	78	
	H2-Rh-H1	31	
	C1-C2-C3-C4	-4	

26	Rh-H1/H2	154/154	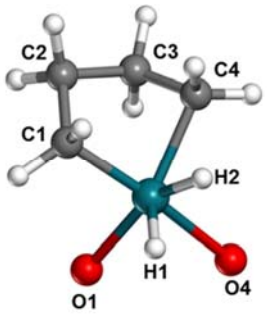
	Rh-C1/C2	206/278	
	Rh-C3/C4	248/209	
	Rh-O1/O4	217/237	
	C1-C2	154	
	C3-C4	151	
	C2-C3	155	
	H1-H2	156	
	H2-Rh-H1	61	
	C1-C2-C3-C4	-37	
	C4-H2	187	
26-27	Rh-H1/H2	154/155	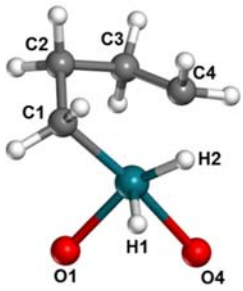
	Rh-C1/C2	206/279	
	Rh-C3/C4	249/210	
	Rh-O1/O4	218/236	
	C1-C2	154	
	C3-C4	152	
	C2-C3	155	
	H1-H2	163	
	H2-Rh-H1	64	
	C4-H2	176	
	C1-C2-C3-C4	-37	
27	Rh-H1/H2	153/171	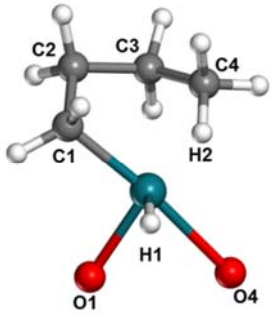
	Rh-C1/C2	205/279	
	Rh-C3/C4	256/231	
	Rh-O1/O4	209/237	
	C1-C2	153	
	C3-C4	153	
	C2-C3	155	
	C4-H2	121	
	C1-C2-C3-C4	-39	
4-28	Rh-H1/H2	159/154	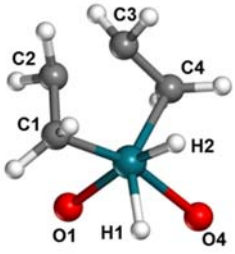
	Rh-C1/C2	202/237	
	Rh-C3/C4	244/208	
	Rh-O1/O4	235/228	
	C1-C2	150	
	C3-C4	147	
	C2-C3	177	
	H1-H2	196	
	H2-Rh-H1	78	

28	Rh-H1/H2	163/164	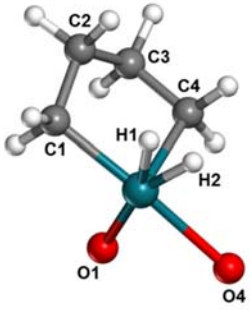
	Rh-C1/C2	208/292	
	Rh-C3/C4	289/206	
	Rh-O1/O4	216/232	
	C1-C2	153	
	C3-C4	152	
	C2-C3	153	
	H1-H2	93	
	C1-H1	220	
	H2-Rh-H1	33	
	C1-C2-C3-C4	-55	
28-29	Rh-H1/H2	155/156	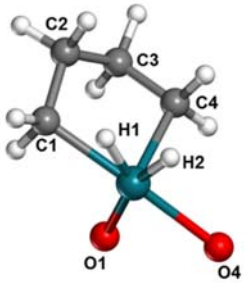
	Rh-C1/C2	216/299	
	Rh-C3/C4	289/206	
	Rh-O1/O4	227/223	
	C1-C2	153	
	C3-C4	152	
	C2-C3	153	
	H1-H2	135	
	C1-H1	165	
	H2-Rh-H1	52	
	C1-C2-C3-C4	-55	
29	Rh-H1/H2	172/154	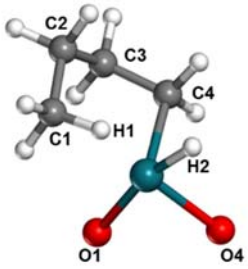
	Rh-C1/C2	238/310	
	Rh-C3/C4	288/205	
	Rh-O1/O4	236/212	
	C1-C2	153	
	C3-C4	152	
	C1-H1	120	
	C2-C3	153	
5-30	Rh-H1/H2	189/154	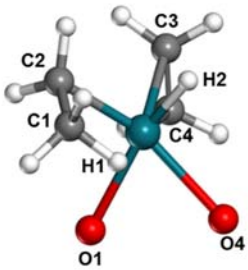
	Rh-C1/C2	234/203	
	Rh-C3/C4	212/216	
	Rh-O1/O4	232/234	
	C1-C2	150	
	C3-C4	140	
	C1-H1	118	
	C4-H2	220	
	C2-C3	295	
	C2-C4	348	
	C2-Rh-C3/C4	90/114	
30	Rh-H1/H2	190/154	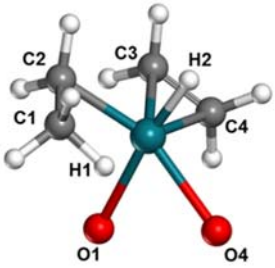
	Rh-C1/C2	236/205	
	Rh-C3/C4	213/211	
	Rh-O1/O4	233/228	
	C1-C2	149	
	C3-C4	141	
	C1-H1	117	
	C2-C3	275	
	C2-C4	362	
	Rh-C2-C1	82	
	C1-C2-C3-C4	2	

30-29	Rh-H1/H2	212/154	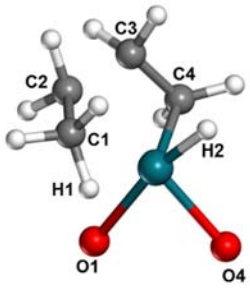
	Rh-C1/C2	243/229	
	Rh-C3/C4	237/200	
	Rh-O1/O4	233/213	
	C1-C2	156	
	C3-C4	149	
	C1-H1	112	
	C2-C3	177	
	C1-C2-C3-C4	65	
	Rh-C2-C1/C4	110	
	C1-C2-C3-C4	83	
30-31	Rh-H1/H2	300/154	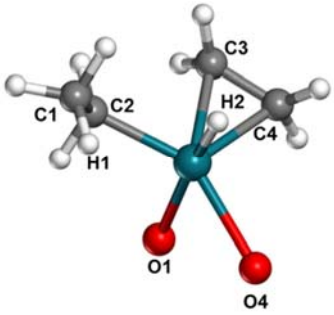
	Rh-C1/C2	296/207	
	Rh-C3/C4	210/208	
	Rh-O1/O4	231/224	
	C1-C2	151	
	C3-C4	142	
	C1-H1	110	
	C2-C3	264	
	C2-C4	355	
	C1-C2-C3-C4	83	
	Rh-C2-C1	110	
	H2-Rh-C2-C1	-30	
31	Rh-H1/H2	327/154	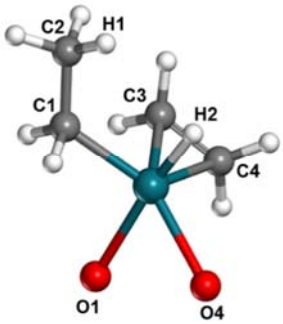
	Rh-C1/C2	312/203	
	Rh-C3/C4	209/207	
	Rh-O1/O4	231/225	
	C1-C2	151	
	C3-C4	143	
	C1-H1	110	
	C2-C3	262	
	C2-C4	353	
	C1-C2-C3-C4	124	
	Rh-C2-C1	124	
	H2-Rh-C2-C1	17	

31-32	Rh-H1/H2	320/154	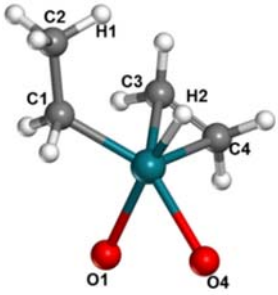
	Rh-C1/C2	316/203	
	Rh-C3/C4	209/207	
	Rh-O1/O4	232/224	
	C1-C2	152	
	C3-C4	143	
	C2-C3	263	
	C1-C2-C3-C4	132	
	H2-Rh-C2-C1	19	
32	Rh-H1/H2	331/154	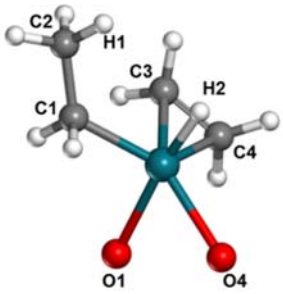
	Rh-C1/C2	316/203	
	Rh-C3/C4	209/207	
	Rh-O1/O4	232/224	
	C1-C2	151	
	C3-C4	143	
	C2-C3	263	
	C1-C2-C3-C4	145	
	H2-Rh-C2-C1	29	
32-33	Rh-C1/C2	357/225	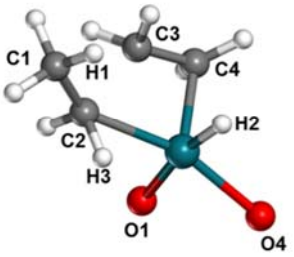
	Rh-C3/C4	226/202	
	Rh-O1/O4	233/214	
	C1-C2	152	
	C3-C4	146	
	C2-C3	190	
	C1-C2-C3-C4	159	
	Rh-H3	209	
	C2-H3	112	
	Rh-H2	154	
33	Rh-H2	154	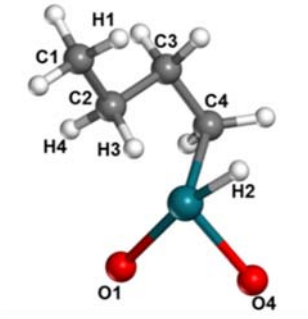
	Rh-C1/C2	367/235	
	Rh-C3/C4	268/203	
	Rh-O1/O4	234/211	
	C1-C2	153	
	C3-C4	151	
	C2-C3	154	
	C1-C2-C3-C4	163	
	Rh-H3/H4	173/266	
	C2-H3/H4	120/110	
33-34	Rh-H1/H2	450/154	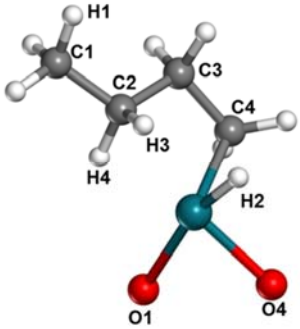
	Rh-C1/C2	388/241	
	Rh-C3/C4	274/204	
	Rh-O1/O4	236/206	
	C1-C2	153	
	C3-C4	152	
	C2-C3	154	
	C1-C2-C3-C4	167	
	Rh-H3/H4	226/211	
	C2-H3/H4	112/113	
	Rh-H2	154	

34	Rh-H1/H2	446/154	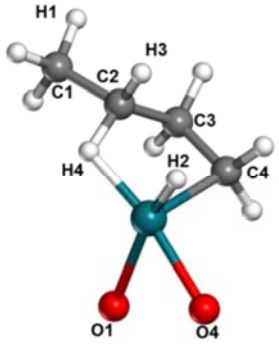
	Rh-C1/C2	364/238	
	Rh-C3/C4	262/204	
	Rh-O1/O4	236/210	
	C1-C2	153	
	C3-C4	151	
	C2-C3	155	
	C1-C2-C3-C4	-166	
	Rh-H3/H4	281/174	
	C2-H3/H4	110/120	
34-35	Rh-H2	154	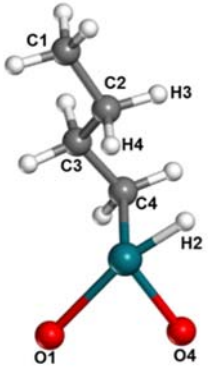
	Rh-C1/C2	450/310	
	Rh-C3/C4	270/201	
	Rh-O1/O4	235/205	
	C1-C2	153	
	C3-C4	152	
	C2-C3	154	
	C1-C2-C3-C4	169	
	Rh-H4	264	
	C2-H4	111	
35	Rh-H1/H2	166/154	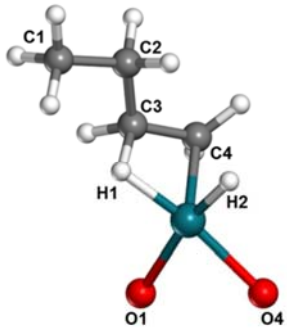
	Rh-C1/C2	403/332	
	Rh-C3/C4	221/202	
	Rh-O1/O4	232/211	
	C1-C2	153	
	C3-C4	147	
	C2-C3	153	
	C1-C2-C3-C4	-161	
	C3-H1	130	
35-36	Rh-H1/H2	157/154	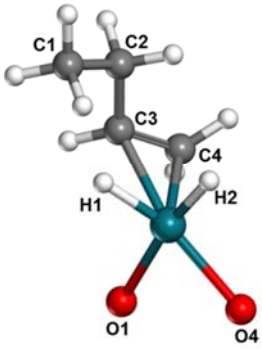
	Rh-C1/C2	387/324	
	Rh-C3/C4	217/205	
	Rh-O1/O4	232/215	
	C1-C2	144	
	C3-C4	153	
	C2-C3	152	
	C1-C2-C3-C4	155	
	C3-H1	160	

36	Rh-H1/H2	159/158	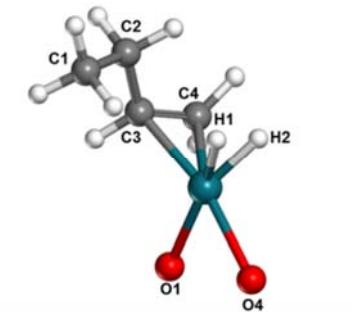
	Rh-C1/C2	364/315	
	Rh-C3/C4	215/210	
	Rh-O1/O4	217/218	
	C1-C2	153	
	C3-C4	141	
	C2-C3	151	
	H1-H2	107	
	C1-C2-C3-C4	147	
	C3-H1	251	
37	Rh-H1/H2	161/162	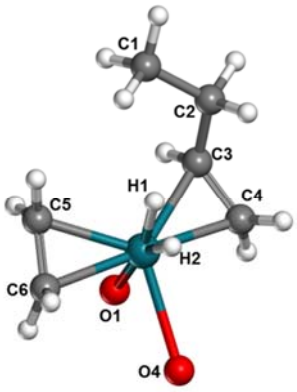
	Rh-C1/C2	367/322	
	Rh-C3/C4	224/218	
	Rh-C5/C6	218/218	
	Rh-O1/O4	216/246	
	C1-C2	153	
	C3-C4	140	
	C2-C3	151	
	C5-C6	140	
	C1-C2-C3-C4	-144	
	H1-H2	97	
38	Rh-H1/H2	496/543	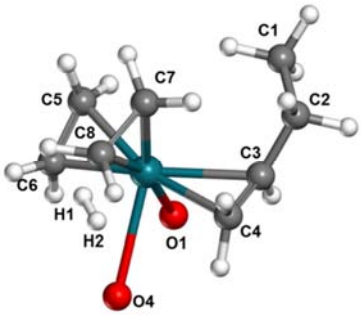
	Rh-C1/C2	363/335	
	Rh-C3/C4	237/225	
	Rh-C5/C6	220/218	
	Rh-C7/C8	210/213	
	Rh-O1/O4	231/265	
	C1-C2	153	
	C3-C4	138	
	C2-C3	150	
	C5-C6	139	
	C7-C8	141	
	C1-C2-C3-C4	-135	
	H1-H2	75	
39	Rh-C1/C2	365/335	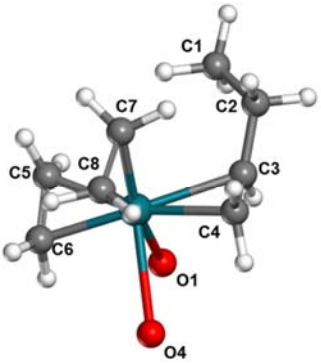
	Rh-C3/C4	237/225	
	Rh-C5/C6	220/217	
	Rh-C7/C8	213/210	
	Rh-O1/O4	231/262	
	C1-C2	153	
	C3-C4	138	
	C2-C3	150	
	C5-C6	140	
	C7-C8	141	
	C1-C2-C3-C4	-136	

Section S6. The 5T cluster model used for the partial normal mode analysis

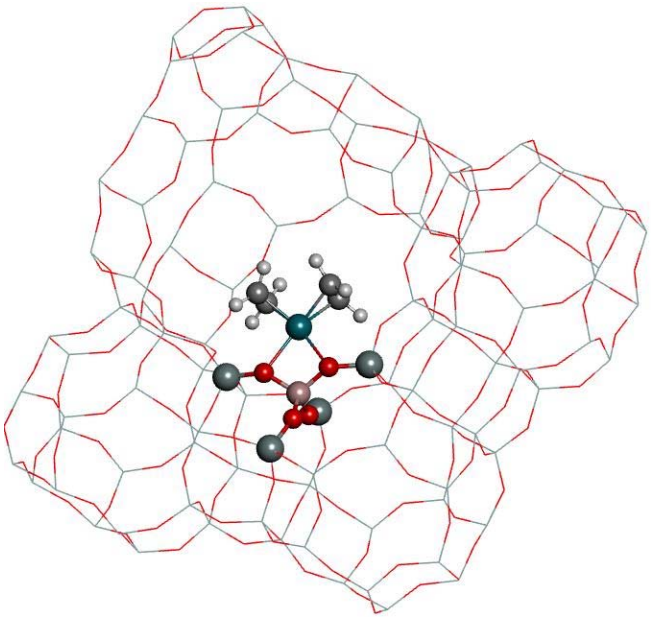

Figure S7. Representation of the 5T cluster (rendered as balls and sticks) used for the partial normal mode analysis. The remaining part of the zeolite framework is kept frozen.

Section S7 Cartesian coordinates of all intermediates and transition states

Provided as a separate archive.